Computer Simulations of Membrane Protein Folding: Structure and Dynamics

C.-M. Chen and C.-C. Chen
Physics Department, National Taiwan Normal University, Taipei, Taiwan, Republic of China

ABSTRACT A lattice model of membrane proteins with a composite energy function is proposed to study their folding dynamics and native structures using Monte Carlo simulations. This model successfully predicts the seven helix bundle structure of sensory rhodopsin I by practicing a three-stage folding. Folding dynamics of a transmembrane segment into a helix is further investigated by varying the cooperativity in the formation of α helices for both random folding and assisted folding. The chain length dependence of the folding time of a hydrophobic segment to a helical state is studied for both free and anchored chains. An unusual length dependence in the folding time of anchored chains is observed.

INTRODUCTION

The three dimensional structures of proteins play an important role in determining their biological functions. Although tremendous efforts have been invested in studying the protein folding problem, the folding kinetics is so far unclear and protein structures are difficult to predict (Bryngelson and Wolynes, 1989; Leopold et al., 1992; Wolynes et al., 1995; Gutin et al., 1996; Li et al., 1996; Chan and Dill, 1997; Onuchic et al., 1997; Duan and Kollman, 1998). Recently, considerable attention has been focused on the cooperatively kinetic behavior of protein folding (Chan, 2000; Kaya and Chan, 2000; Fan et al., 2001). Kaya and Chan (2000) have shown the lack of cooperativity in popular lattice models, such as the two-letter HP model or the twenty-letter model, by using the calorimetric criterion. This may be due to oversimplification of these lattice models in both chain representations and intrachain interactions. Although these coarse-grained lattice models have the advantage of cutting computational efforts in studying protein folding, the kinetic information on the evolution of a protein chain from one coarse-grained structure to another is also lost. It is quite possible that some kinetic pathway is overwhelmingly enhanced or entirely blocked due to intermolecular interactions or molecular packing. A possible origin of this effect is the dipole-dipole interactions between amide groups in real α helices (Cantor and Schimmel, 1980). However the resolution of coarse-grained lattice models is not enough to distinguish these pathways. Lattice models also tend to use statistical contact potentials extracted from the Protein Data Bank (PDB), which provide little information about how these potentials arise from realistic physical interactions. It is also unclear how these potentials would evolve when the protein structure deviates from its native structure.

Membrane proteins (MPs) perform important and diverse functions in living cells, such as regulation, communication, and assisting the folding of other MPs (for a review, see White and Wimley, 1999). They are partially buried in the nonpolar environment of a lipid bilayer, where the hydrophobic effect is absent. Because lipid tails are unable to form hydrogen bonds with proteins, the intrachain hydrogen bonding along the backbone of proteins in a membrane plays a significant role in forming their native structure. According to the structure of transmembrane segments, there are two known classes of MPs. The first class contains MPs whose transmembrane segments all form an α-helical structure with lengths (N_c) of 17 to 25 amino acids (aa). In the second class, on the other hand, those MPs usually have a β-barrel structure. However, due to difficulties in crystallizing MPs, only a dozen or so MPs have known crystallographic structures so far. Among them, helix bundles are much more abundant than β barrels.

A previous model using a full-backbone atom representation in a diamond lattice initiates an interesting study on the insertion of polypeptides into a membrane (Milik and Skolnick, 1992). This model explicitly specifies that hydrogen bonds can form for only $(i, i \pm 4)$ pairs, where i labels amino acids in the chain. This can be considered as an extreme case in emphasizing the $(i, i \pm 4)$ hydrogen bonding state because there is no reason to forbid hydrogen bonding between $(i, i \pm n)$ residues for $n > 4$. Furthermore, this restriction also excludes the possibility to form β strands. Our previous paper (Chen, 2001) proposes a lattice model for the folding of transmembrane polypeptides, in which the backbone hydrogen bonding of polypeptides can occur between i and $i \pm n$ for $n \geq 4$. Our model predicts two possible stable structures of transmembrane polypeptides, including helix and double helix structures, which have been observed for gramicidin dimers (Arumugam et al., 1996). However, the folding time of a polypeptide chain in this simple model is unexpectedly long, which might result from its incapability to distinguish the differences among various hydrogen bonding states. In this paper, we propose a lattice model of MPs to study their native structures and cooperative folding.

Submitted August 23, 2002, and accepted for publication October 31, 2002.

Address reprint requests to Chi-Ming Chen, 88 Sec. 4 Ting-Chou Rd., Taipei, Taiwan, 11718. Tel.: 886-2-86638109; E-mail: cchen@phy.ntnu.edu.tw.

0006-3495/03/03/1902/07 $2.00

The main goal of our model is to predict the native structures of membrane proteins by their relevant physical interactions alone, and this model is then reliable for us to study the folding kinetics of a transmembrane peptide with minimal artifacts. Predicted structures of MPs from our model can be refined by all-atom models and will be useful in studying their biological functions by docking studies. This model has a composite energy function to describe interactions among amino acids, which uses realistic interactions when residues are in a membrane but statistical potentials when they are in water. We show that this model predicts a reasonably good native structure of sensory rhodopsin I (SRI), which is a phototaxis receptor in Halobacterium salinarum and consists of 239 amino acids. In addition, we study the cooperative effect on the folding time of MPs by introducing a cooperative factor to favor the $(i, i \pm 4)$ hydrogen bonding state. Our chain representation is based on the bond-fluctuation model (Carmesin and Kremer, 1988; Chen and Fwu, 2001; Chen, 2001), which has advantages of giving reasonably good secondary structures and of simulating a more realistic diffusive kinetics than regular lattice models, while the computational cost is still quite limited compared to that of off-lattice models. We note that, although a helix bundle structure is studied in this paper, our model can also be used to predict β-barrel structures because backbone hydrogen bonding is possible for amino acids far apart from each other in the sequence.

MODEL

In our model, the potential energy U of MPs can be expressed as $U = U_{\text{membrane}} + U_{\text{water}}$, where U_{membrane} and U_{water} are the potential energies of MPs in a membrane and in water, respectively. The simulation box is divided into three regions including two water phases separated by a hydrocarbon (membrane) phase of thickness L. For amino acids within the membrane, their potential energy is given by $U_{\text{membrane}} = E_{\text{H-bond}} + E_{\text{bend}} + E_{\text{vdw}}$, where $E_{\text{H-bond}}$ is the hydrogen bonding energy, E_{bend} is the bending energy of the chain, and E_{vdw} is the van der Waals (vdW) interaction between amino acids. A hydrogen bond can form if two amino acids are separated by four lattice spacing (or 5.4 Å). However, each amino acid can at most participate in two hydrogen bonds. Moreover, hydrogen bonding is highly directional and has a maximal strength when N—H and O═C bonds are co-linear. Therefore we model the hydrogen bonding energy by $E_{\text{H-bond}} = \sum_{\langle i,j \rangle} |(\mathbf{n}_i \bullet \mathbf{r}_{ij})\,(\mathbf{n}_j \bullet \mathbf{r}_{ij})|\,\delta_{r(i,j),4}$, where $\mathbf{n}_i$ is the N—H (or O═C) bond orientation of the i-th amino acid, while $r(i, j)$ and $\mathbf{r}_{ij}$ are the distance and its unit vector between amino acids i and j. Because the backbone hydrogen bonding is the dominant interaction for the formation of secondary structures of MPs, its energy strength is set to unity. Furthermore, we have explicitly excluded the possibility of forming 2_7 ribbons and 3_{10} helices due to steric hindering by disallowing the hydrogen bonding between $(i, i \pm 2)$ and $(i, i \pm 3)$ pairs. The bending energy of the chain is assumed to be $e_1 \sum_i (1 - \cos\theta_i)$, where e_1 is the bending rigidity and θ_i is the angle between two consecutive bonds i and $i + 1$. The vdW interaction between amino acids is modeled by $E_{\text{vdw}} = e_2 \sum_{\langle i,j \rangle} \{[1.78/r(i, j)]^{12} - [1.78/r(i, j)]^6\}$, where e_2 is its strength relative to hydrogen bonding. This vdW term has a minimum if two amino acids are next to each other in a cubic lattice model. For amino acids in water, their interactions are modeled by a residue-residue contact potential (E_{contact}) and the hydropathical interaction ($E_{\text{hydropathy}}$), i.e., $U_{\text{water}} = E_{\text{contact}} + E_{\text{hydropathy}}$. The interactions between the exposed residues and the lipid bilayer are ignored. Here we use the Thomas-Dill contact potential with strength e_3 to model the residue-residue interaction in water when residues are in contact (Thomas and Dill, 1996). Because MP residues exposed to water are mostly exterior residues, the positive contact energies between exterior residues in this potential imply highly dynamical loops of MPs in the water phase. The hydropathical interaction of amino acids in water can be modeled by using a rescaled Kyte-Doolittle hydrophathy index (spread between -1 and 1) with strength e_4, which is mainly determined by the Gibbs free energy change for transferring amino acids from water into condensed vapor (Kyte and Doolittle, 1982). In addition, the insertion of a polypeptide chain into a membrane will disturb the integrity of the membrane and local lipid density around the chain, which increases the energy of the membrane (White and Wimley, 1999). We model this effect by introducing an effective lateral pressure (P) applied to the polypeptide chain to minimize its lateral area ($A = \sum_i l_i^2$) in the membrane, where l_i is the projected length of the i-th transmembrane segment on the membrane surface (Chen, 2001). Therefore, to find the ground state structure of MPs, the relevant physical quantity to be minimized in our model is the enthalpy $H = U + PA$.

ALGORITHM OF SIMULATIONS

The bond fluctuation model is an efficient method of simulating the dynamics of polymer chains. It was originally introduced by Carmesin and Kremer (1988) for studying dynamics of polymer chains in various spatial dimensions. Since then it has been used for investigation of the crossover between Rouse and reptation dynamics (Gerroff et al., 1993), for studying interdiffusion of polymer blends (Deutsch and Binder, 1991), the dynamics of polymer melts near glass transition (Ray et al., 1993), and polymer crystallization in dilute solution (Chen and Higgs, 1998).

Each monomer in the model is a cube of length 1 (lattice spacing) on a cubic lattice as shown in Fig. 1. The set of allowed bond vectors is $\mathrm{B} = \mathrm{P}(2,0,0) \cup \mathrm{P}(2,1,0) \cup \mathrm{P}(2,1,1) \cup \mathrm{P}(2,2,1) \cup \mathrm{P}(3,0,0) \cup \mathrm{P}(3,1,0)$, where $\mathrm{P}(a,b,c)$ stands for the set of all permutations and sign combinations of $\pm a$, $\pm b$, $\pm c$. The number of configurations per bond is $z = 108$. The length of one bond can take any one of the five values $2, 5^{1/2}, 6^{1/2}, 3, 10^{1/2}$ (in units of lattice spacing). Chains satisfy the excluded volume constraint: no lattice site may be occupied by more than one monomer. The set B is chosen to satisfy the constraints of both excluded volume between monomers and topological

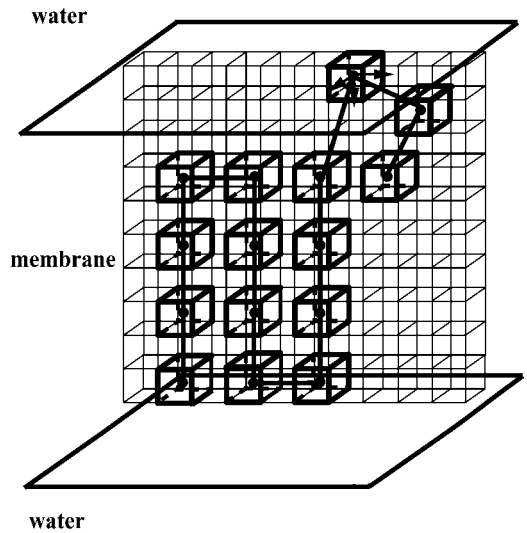

FIGURE 1 One protein chain of 15 residues confined in a membrane is shown. The membrane phase separates two water phases. All residues are shown in one plane for convenience, although the simulations are done in three dimensions.

entanglement between chains (i.e., two chains cannot pass through each other). If any other bond vectors were added to this set, some chains would become ''phantom'' chains.

To study the structure and folding dynamics of MPs, a protein chain is represented by the bond-fluctuation model, and its folding is simulated by the Metropolis Monte Carlo (MC) algorithm in a cubic lattice at a constant temperature T. At each instant, a residue is picked up at random and attempts to move in any of the six directions by one lattice spacing. If any attempted move of residues satisfies the excluded volume constraint and the new bond vectors are still in the allowed set, then the move is accepted with probability $p = \min[1, \exp(-\Delta H/T)]$, where ΔH is the enthalpy change of the system.

RESULTS AND DISCUSSION

Folding structures

First, we apply this lattice model to study the thermodynamic ground state structure of SRI. A previous attempt to simulate the folding of SRI with an arbitrary initial configuration in the water phase did not reach the ground state for two reasons: 1) the partition of the chain into several transmembrane segments took a long computer time because hydrophilic residue could not cross the energetic barrier (Milik and Skolnick, 1992), and 2) the packing of transmembrane segments is much slower than the formation of each individual helix. Therefore we simulate the folding of SRI according to a three-stage model, which is an extension of the two-stage model (Popot and Engelman, 1990). This model is consistent with observed facts, including the nature of transmembrane segments in known structures, refolding experiments, the assembly of integral membrane from fragments, and the existence of very small integral membrane protein subunits. The physical picture of membrane protein folding proposed here is that a dominant hydrophobic interaction at early times hides the hydrophobic segments from water, followed by backbone hydrogen bonding assisted helix formation (a local interaction in sequence), and finally the packing of helices due to the vdW interaction (a nonlocal interaction in sequence). At the first stage, the chain is partitioned into several transmembrane segments by its hydropathy. Each segment then folds to form a secondary structure to optimize the hydrogen bonding along the backbone during the second stage. Finally, these autonomous folding domains will aggregate to form a compact structure due to the vdW interaction.

During the first stage, as shown in Fig. 2, the average hydropathy index of SRI using a window of 20 amino acids is calculated. To optimize the hydropathical interaction, the center of a transmembrane segment of 20 amino acids is located at those higher peaks of the hydropathy profile. Because no overlap is allowed for two segments, seven transmembrane segments are predicted for SRI from the first stage. The inset of Fig. 2 shows the reduction in hydrophobic energy when those transmembrane segments are placed in the membrane phase for various window sizes. The hydrophobic energy can be further reduced if the window size of each transmembrane segment is variable. This

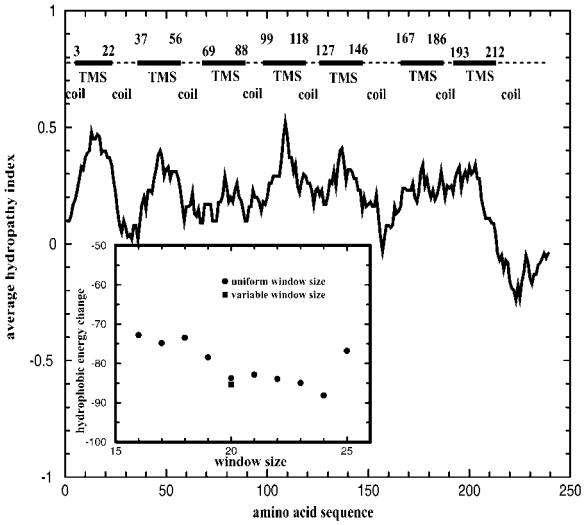

FIGURE 2 The average hydropathy index of SRI for a window of 20 amino acids. Seven transmembrane segments (TMSs) are predicted for SRI from optimizing the hydropathical interaction. The schematic representation of SRI above the hydropathy profile shows seven TMSs (*filled rectangles*) and eight coils (*dash lines*). The inset shows the hydrophobic energy reduction for various window sizes. Filled circles are results from using uniform window size ranging from 16 to 25. The filled square is a further minimization of the hydrophobic energy by varying the length of each transmembrane segment obtained from using window size 20.

prediction is used to produce an initial configuration of SRI to perform MC simulations of its folding at the second stage: seven transmembrane segments are randomly distributed in the membrane phase, and two neighboring segments are connected by a random coil. The folding of the entire chain is simulated at this stage to optimize the enthalpy of the system. The result of the second stage is not sensitive to the window size used at the first stage. In fact, it remains the same even when only thirteen residues of each segment are placed in the membrane initially. Here we choose $e_1 = 0.3$, $e_2 = 0$, $e_3 = 0.3$, $e_4 = 1.5$, $P = 0.1$, and $L = 23$ lattice spacing ($\sim$31 Å, White and Wimley, 1999). The choice of these parameters is not unique. Because all interactions in our model are weak forces, we expect these energetic parameters to be of the same order of magnitude (the strength of hydrogen bonding is taken to be of order 1). No drastic changes in the secondary structure of SRI are observed if a slightly different set of parameters is used. We note that, to obtain a better representation of α helices, the values of bending rigidity and lateral pressure adopted here are different from those in our previous study (Chen, 2001). However the general features of folding dynamics and structure in this case are not affected. During this stage, the vdW interaction is switched off and the secondary structure formation is dominated by the hydrogen bonding and the hydropathical interaction. In Fig. 3, we show the comparison of the PDB secondary structure of SRI (A) (Berman et al., 2000) to our predicted structures for $L = 23$ (B) and $L = 24$

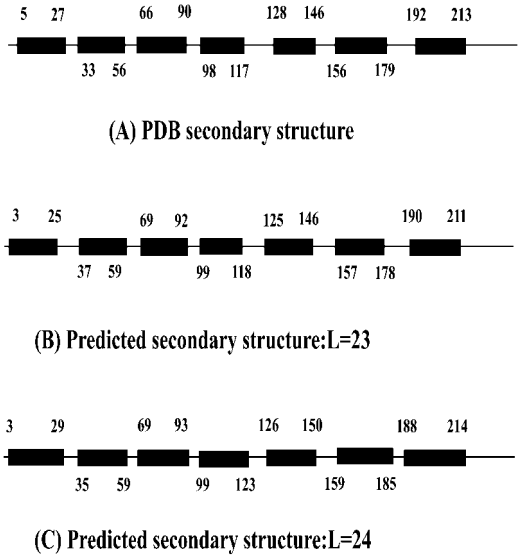

FIGURE 3 A comparison of the PDB secondary structure (A) and our predictions of SRI for $L = 23$ (B) and $L = 24$ (C). Each helix is represented by a filled rectangle. Those numbers along the chain label the corresponding amino acids at both ends of transmembrane helices. The parameters used are $e_1 = 0.3$, $e_2 = 0$, $e_3 = 0.3$, $e_4 = 1.5$, $P = 0.1$.

(C). Both simulations predict a seven-helix structure of SRI. The average helix length of SRI is 22.4 aa in the PDB structure, and is 22.3 aa for $L = 23$ and 25.9 aa for $L = 24$. For $L = 23$, the prediction error in the average helix length is 0.6%, and the secondary structure alignment error (mismatch between Fig. 3 A and 3 B) is 11.3%. When the membrane thickness varies slightly, the seven-helix structure of SRI is still stable, but the helix regions will change correspondingly. For $L = 24$, its deviation from the PDB structure is 15.3% in the average helix length and is 17.6% in their mismatch. After the formation of all autonomous folding domains, we switch on the vdW interaction and switch off all other interactions. During this association stage, the initial configuration of SRI is taken from results at the second stage and each helix can only diffuse within the membrane (neighboring helices are constrained by their connecting loop). Packing of helices is a result of the vdW interaction alone. The external work done by the effective lateral pressure in our model does not drive helices to pack, because the helical structure (or projected area) of each transmembrane segment is fixed at this stage. Fig. 4 shows a comparison of our predicted tertiary structure (A) (only helical regions are shown) with the PDB structure (B). The resemblance of these two structures demonstrates the validity of our model in predicting the native structure of MPs. We note that tilting and distortion of transmembrane helices can be better studied in an off-lattice model, and the results will appear elsewhere (Chen and Chen, in preparation). Such a coarse-grained structure can be used as the initial configuration in an all-atom simulation or minimization to obtain a good native structure.

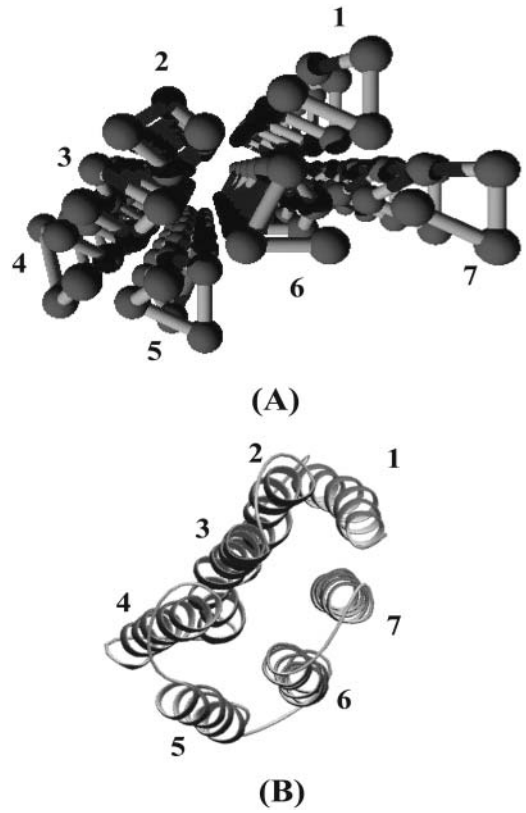

FIGURE 4 A comparison of the PDB tertiary structure (A) and our prediction (B) of SRI. Seven helices are labeled according to their position along the sequence. Flexible regions of SRI are not shown in (A). The parameters used are $e_1 = 0.3$, $e_2 = 0.3$, $e_3 = 0.3$, $e_4 = 1.5$, $P = 0.1$.

Folding dynamics of a transmembrane segment

After successfully predicting the native structure of SRI without using constraints from experimental data, we believe that those interactions in our model should dominate the folding process of MPs and that our model is suitable for studying their folding dynamics. Therefore, our model might provide new perspectives that are different from those of existing models (Milik and Skolnick, 1992, 1993, 1995). An important question in studying protein folding dynamics concerns the cooperative effect in α-helix formation. As indicated from the Ramanchandran plot, the formation of idealized helices strongly depends on the backbone structures (Mathews and van Holde, 1996); if the number of amino acids per turn is greater than four, no ideal helical structure can form. Therefore, the cooperative effect of helices resulting from the steric hindrance of the backbone structure would favor the formation of $(i, i \pm 4)$ hydrogen bonding over the others. For MPs, another feasible origin of cooperativity is membrane-promoting α-helix formation, which has been studied by both experiments and simulations (Deber and Li, 1995; Deber and Goto, 1996; Efremov et al., 1999). Because our previous study (Chen, 2001) allows all

(i, $i \pm n$) hydrogen bonding for $n \geq 4$, our previous model has no cooperative effect and leads to an exponential growth of the folding time for helix formation as the helix length increases. To properly include the cooperative effect of (i, $i \pm 4$) hydrogen bonding, here we add an extra favorable factor $\exp(\alpha\Delta h)$ in the moving probability of each residue to enhance the cooperative helix formation, where Δh is the change of (i, $i \pm 4$) hydrogen bonding pairs and α is the cooperative factor. This cooperative effect on the folding time of a single transmembrane helix (AVATAYLGGA-VALIVGVAFVWLLY, a transmembrane helix of SRI) has been studied for both random folding (with a random initial configuration) and assisted folding (with a parallel initial configuration to the membrane normal) using $e_1 = 0.3$, $e_2 = 0$, $e_3 = 0.3$, $e_4 = 1.5$, $P = 0.1$, $T = 0.31$ (the optimal folding temperature), and $L = 24$. The assisted folding is to mimic the helix formation of a hydrophobic segment assisted by a hydrophilic channel. This particular initial configuration selects a folding pathway with a smaller activated energy barrier than a random initial configuration, as described in our previous work (Chen, 2001). It is found that the mean first passage time (MFPT) to a helical state is minimized at $\alpha \cong 1.2$ for both cases, as shown in Fig. 5. The folding time to a helical state increases exponentially if α deviates from this optimized value. For smaller values of α, the chain is easily trapped at wrongly folded states. If α is too large, the partially folded helix is often trapped at wrong positions in the membrane and the helix formation cannot continue to the rest of the peptide chain due to the presence of the water-membrane interface. These misfolded structures of a frustrated partial helix must be unfolded first before the chain can reach its ground state, which drastically increases the folding time. Note that, however, we do not know whether α is optimized for membrane protein folding or, if it is optimized, why.

To further investigate the folding dynamics of a transmembrane helix at the optimized cooperativity, we calculate the MFPT of polyvalines of various chain lengths. Fig. 6 shows the MFPT as a function of chain length for both free and anchored chains. The anchored chains are fixed on the membrane surface at one end (the fixed end can still diffuse on the surface), whereas both ends of a free chain can move freely. This investigation is particularly useful in understanding the folding dynamics of a hydrophobic helix with one end constrained on the membrane-water interface due to charged amino acids in its sequence. Furthermore, we consider the following two types of N-H bond rotating kinetics: the thermal rotation of the bond orientation is 1) comparable with or 2) much faster than the thermal motion of amino acids. The parameters used here are $e_1 = 0.3$, $e_2 = 0$, $e_3 = 0.3$, $e_4 = 1.5$, $P = 0.1$, $T = 0.31$, and L = 24 (but $L = 26$ for $N_c = 26$ and $L = 28$ for $N_c = 28$). The length dependence of the MFPT is similar for both types of bond rotating kinetics. For N_c ranging from 18 to 28, the MFPT of free chains to a helical state increases roughly linearly with

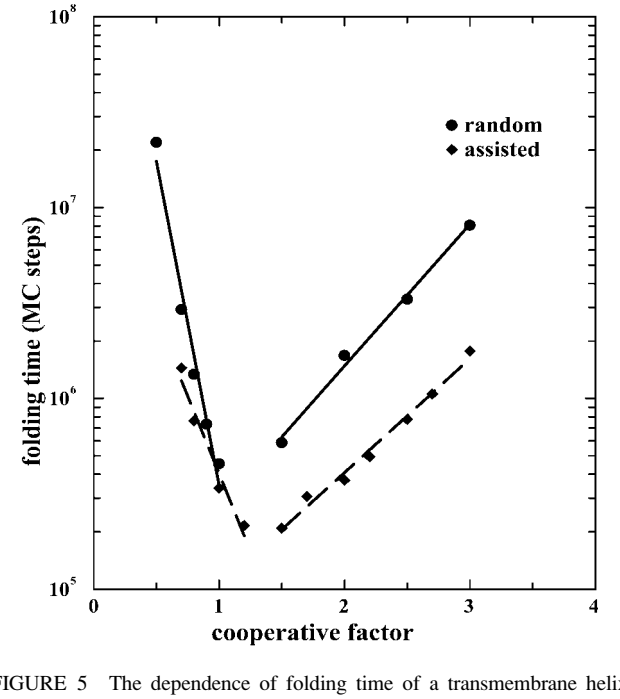

FIGURE 5 The dependence of folding time of a transmembrane helix on cooperative factor for both random folding and assisted folding. The parameters used are $e_1 = 0.3$, $e_2 = 0$, $e_3 = 0.3$, $e_4 = 1.5$, $P = 0.1$, $T = 0.31$, and $L = 24$.

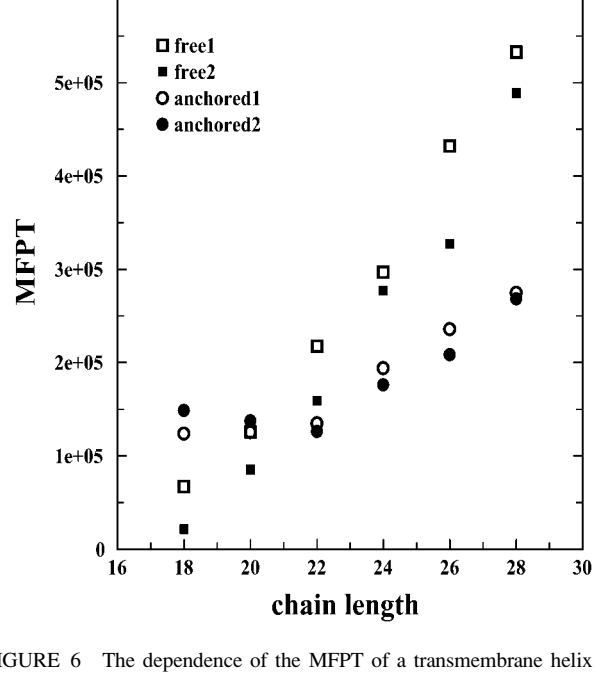

FIGURE 6 The dependence of the MFPT of a transmembrane helix on chain length for both free (*open squares*: rotating kinetics 1; *filled squares*: rotating kinetics 2) and anchored chains (*open circles*: rotating kinetics 1; *filled circles*: rotating kinetics 2). The parameters used are $e_1 = 0.3$, $e_2 = 0$, $e_3 = 0.3$, $e_4 = 1.5$, $P = 0.1$, $T = 0.31$, and $L = 24$.

chain length, which is very different from the nearly exponential growth of the MFPT in our previous study at zero cooperativity (Chen, 2001). This difference is clearly due to the cooperative helix formation. Because the configuration space of a hydrophobic peptide increases drastically with its chain length, the MFPT to search for helical states also increases drastically at zero cooperativity. At the optimal cooperativity, only part of the configuration space near helical states is focused in searching, which leads to a near linear MFPT. For anchored chains, the MFPT decreases slightly for $N_c < 22$ but increases linearly for $N_c \geq 22$. The initial drop in the MFPT of anchored chains is due to the fact that shorter chains have a smaller cooperative effect and thus they might take longer times to fold even when their configuration space is also smaller. Because anchored chains have a smaller configuration space and a larger cooperative effect than free chains, a smaller slope of the MFPT is observed for anchored chains. We note that anchored chains have a larger MFPT than free chains at short chain lengths due to the anchored restriction in their folding pathways.

CONCLUSIONS

In conclusion, we have proposed in this paper a lattice model for membrane protein folding, which correctly predicts the secondary and tertiary structures of SRI at the coarse-grained level based on a three-stage folding hypothesis. The seven-helix structure of SRI is found to be stable if the membrane thickness changes slightly. This model is also used to study the cooperative folding of a hydrophobic helix by introducing a favorable factor $\exp(\alpha\Delta h)$ to α-helical states. We find that the folding time of transmembrane helices is optimized for $\alpha = 1.2$. The polypeptide chains are usually trapped at wrong configurations for small values of cooperativity, whereas they tend to be trapped at wrong positions in the membrane at large cooperativity. The dependence of folding time on chain length is nearly linear for free chains but exhibits an unusual behavior for anchored chains, which might result from the competition between cooperativity and the number of configurations as chain length varies.

We thank K. Dill and T.K. Lee for stimulating discussions.

This work is supported, in part, by the National Science Council of Taiwan under grant no. NSC 90-2112-M-003-024. C.M.C. is grateful for the hospitality at the Department of Pharmaceutical Chemistry, University of California at San Francisco.

REFERENCES

Arumugam, S., S. Pascal, C. L. North, W. Hu, K. C. Lee, M. Cotten, R. R. Ketchem, F. Xu, M. Brenneman, F. Kovacs, F. Tian, A. Wang, S. Huo, and T. A. Cross. 1996. Conformational trapping in a membrane environment: a regulatory mechanism for protein activity? *Proc. Natl. Acad. Sci. U.S.A.* 93:5872–5876.

Berman, H. M., J. Westbrook, Z. Feng, G. Gilliland, T. N. Bhat, H. Weissig, I. N. Shindyalov, and P. E. Bourne.2000. The protein data bank. *Nucleic Acids Res.* 28:235–242.

Bryngelson, J. D., and P. G. Wolynes. 1989. Intermediates and barrier crossing in a random energy model (with applications to protein folding). *J. Phys. Chem.* 93:6902–6915.

Cantor, C. R., and P. R. Schimmel. 1980. Biophysical Chemistry. W. H. Freeman Company, San Francisco. 862–863.

Carmesin, I., and K. Kremer. 1988. The bond fluctuation method: a new effective algorithm for the dynamics of polymers in all spatial dimensions. *Macromolecules.* 21:2819–2823.

Chan, H. S., and K. A. Dill. 1997. Solvation: how to obtain microscopic energies from partitioning and solvation experiments. *Annu. Rev. Biophys. Biomol. Struct.* 26:425–459.

Chan, H. S. 2000. Modeling protein density of states: additive hydrophobic effects are insufficient for calorimetric two-state cooperativity. *Proteins.* 40:543–571.

Chen, C.-M., and P. G. Higgs. 1998. Monte Carlo simulations of polymer crystallization in dilute solution. *J. Chem. Phys.* 108:4305–4314.

Chen, C.-M. 2001. Lattice model of transmembrane polypeptide folding. *Phys. Rev. E Stat. Nonlin. Soft Matter Phys.* 63:010901.

Chen, C.-M., and Y.-A. Fwu. 2001. Monte Carlo simulations of polymer brushes. *Phys. Rev. E Stat. Nonlin. Soft Matter Phys.* 63:011506.

Deber, C. M., and S.-C. Li. 1995. Peptides in membranes: helicity and hydrophobicity. *Biopolymers.* 37:295–318.

Deber, C. M., and N. K. Goto. 1996. Folding proteins into membranes. *Nat. Struct. Biol.* 3:815–818.

Deutsch, H. P., and K. Binder. 1991. Interdiffusion and self-diffusion in polymer mixtures—a Monte Carlo study. *J. Chem. Phys.* 94:2294–2304.

Duan, Y., and P. A. Kollman. 1998. Pathways to a protein folding intermediate observed in a 1-microsecond simulation in aqueous solution. *Science.* 282:740–744.

Efremov, R. G., D. E. Nolde, G. Vergoten, and A. S. Arseniev. 1999. A solvent model for simulations of peptides in bilayers. I. Membrane-promoting α-helix formation. *Biophys. J.* 76:2448–2459.

Fan, K., J. Wang, and W. Wang. 2001. Modeling two-state cooperativity in protein folding. *Phys. Rev. E Stat. Nonlin. Soft Matter Phys.* 64:041907.

Gerroff, I., A. Milchev, K. Binder, and W. Paul. 1993. A new off-lattice Monte-Carlo model for polymers—a comparison of static and dynamic properties with the bond-fluctuation model and application to random media. *J. Chem. Phys.* 98:6526–6539.

Gutin, A. M., V. I. Abkevich, and E. I. Shakhnovich. 1996. Chain length scaling of protein folding time. *Phys. Rev. Lett.* 77:5433–5436.

Kaya, H., and H. S. Chan. 2000. Energetic components of cooperative protein folding. *Phys. Rev. Lett.* 85:4823–4826.

Kyte, J., and R. F. Doolittle. 1982. A simple method for displaying the hydrophobic character of a protein. *J. Mol. Biol.* 157:105–132.

Leopold, P. E., M. Montal, and J. N. Onuchic. 1992. Protein folding funnels—a kinetic approach to the sequence structure relationship. *Proc. Natl. Acad. Sci. USA.* 89:8721–8725.

Li, H., R. Helling, C. Tang, and N. Wingreen. 1996. Emergence of preferred structures in a simple model of protein folding. *Science.* 273:666–669.

Mathews, C. K., and K. E. van Holde. 1996. Biochemistry. Benjamin/Cummings Publishing Co., Menlo Park. 165–174.

Milik, M., and J. Skolnick. 1992. Spontaneous insertion of polypeptide-chains into membranes: a Monte Carlo model. *Proc. Natl. Acad. Sci. USA.* 89:9391–9395.

Milik, M., and J. Skolnick. 1993. Insertion of peptide chains into lipid-membranes: an off-lattice Monte Carlo dynamics model. *Proteins.* 15:10–25.

Milik, M., and J. Skolnick. 1995. A Monte Carlo model of fd and Pfl proteins in lipid membranes. *Biophys. J.* 69:1382–1386.

Onuchic, J. N., Z. Luthey-Schulten, and P. G. Wolynes. 1997. Theory of protein folding: the energy landscape perspective. *Annu. Rev. Phys. Chem*. 48:545–600.

Popot, J. L., and D. M. Engelman. 1990. Membrane protein folding and oligomerization: the two-stage model. *Biochemistry*. 29:4031–4037.

Ray, P., J. Baschnagel, and K. Binder. 1993. Dynamics near the glass-transition in two-dimensional polymer melts: a Monte Carlo simulation study. *J. Phys.: Condens. Matter*. 5:5731–5742.

Thomas, P. D., and K. A. Dill. 1996. An iterative method for extracting energy-like quantities from protein structures. *Proc. Natl. Acad. Sci. USA*. 93:11628–11633.

White, S. H., and W. C. Wimley. 1999. Membrane protein folding and stability: physical principles. *Annu. Rev. Biophys. Biomol. Struct*. 28:319–365.

Wolynes, P. G., J. N. Onuchic, and D. Thirumalai. 1995. Navigating the folding routes. *Science*. 267:1619–1620.